Low-Frequency Conductivity Due to Hopping Processes in Silicon

M. POLLAK* AND T. H. GEBALLE
Bell Telephone Laboratories, Murray Hill, New Jersey
(Received February 1, 1961)

The complex conductivity has been measured in n-type silicon with various kinds of impurities at frequencies between 10^2 and 10^5 cps and temperatures between 1 and 20°K. In most cases it is orders of magnitude larger than the measured dc conductivity and is attributed to polarization caused by hopping processes. The observed frequency dependence in the measured range can be expressed as $A\omega^{0.8}$, where A is a complex constant. At the low-temperature end the conductivity is roughly proportional to minority impurity concentration and is almost independent of the majority impurity concentration and At higher temperatures the conductivity becomes approximately proportional to the product of both concentrations. A simple theory, based on the currently accepted model of impurity conduction, is given for the higher temperature range. It accounts well for the observed frequency and concentration dependences. However, only order-of-magnitude absolute agreement is obtained.

I. INTRODUCTION

SINCE Hung and Gleissman[1] first observed a new conduction mechanism in their low-temperature investigation of Ge, a considerable number of papers have been published on the topic.[2–15] The accepted term for this conduction mechanism has become impurity conduction. All the investigations have been concerned with transport resulting from the application of steady fields. Most theoretical workers on impurity conduction used essentially the model introduced by Conwell and Mott. The more refined theories[9,12] are in good agreement with the published experimental results, and hence we can hope that the model is realistic. According to that model which is valid for low concentrations, the transport occurs by electrons hopping between states which are essentially localized around acceptor or donor impurities. For such a hopping to take place it is necessary for some of the localized states to be vacant and hence compensation of the majority impurity becomes an essential feature of impurity conduction. This indeed has been demonstrated by Fritzsche.[8] Because of the Coulombic forces between the ionized impurities, the state of lowest energy is achieved when the majority impurity nearest to a given minority impurity is ionized, as illustrated in Fig. 1. On application of a steady electric field a current can be perpetuated only if thermal energy is sufficient to overcome the Coulombic potential around the minority impurity. On the other hand, even if there is insufficient thermal energy, the potential is altered by the applied electric field and a new equilibrium has to be established. This will take a time of the order of the hopping time and a net polarization will occur. The rate of polarization can be detected as a current in an ac experiment. The fact that such an experiment

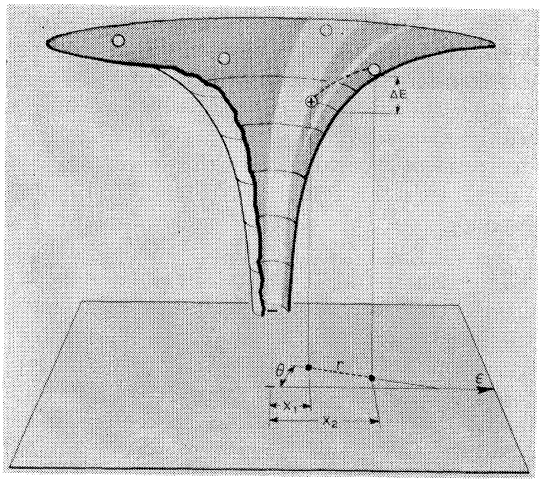

FIG. 1. A two-dimensional representation of the Mott-Conwell model for impurity conduction. The upper half of the figure shows a random distribution of majority donor atoms in the Coulombic potential of the negatively charged acceptor. The charge distribution can respond to an applied field ϵ by an electron hop (with energy increase ΔE) from an adjacent uncharged donor to the charged donor as indicated by the dashed line. The lower half of the figure shows the impurity atoms projected on the plane containing the field ϵ and illustrates the notation used in the text. Ionized donors and acceptors are represented by plus and minus signs; neutral donors by open circles.

* Present address: Westinghouse Research Laboratories, Pittsburgh, Pennsylvania. Part of this work has been performed while at the present address.

[1] C. S. Hung and J. R. Gleissman, Phys. Rev. **79**, 726 (1950).
[2] H. Fritzsche and K. Lark-Horowitz, Physica **20**, 834 (1954).
[3] E. M. Conwell, Phys. Rev. **103**, 51 (1956).
[4] N. F. Mott, Can. J. Phys. **34**, 1356 (1956).
[5] P. J. Price, IBM J. of Research Develop. **2**, 123 (1958).
[6] R. Keyes and R. J. Sladek, J. Phys. Chem. Solids **1**, 143 (1956).
[7] S. H. Koenig and G. Gunther Mohr, J. Phys. Chem. Solids **2**, 268 (1957).
[8] H. Fritzsche, J. Chem. Phys. Solids **6**, 69 (1958); **8**, 257 (1959); Phys. Rev. **119**, 1899 (1960).
[9] T. Kasuya and S. Kiode, J. Phys. Soc. Japan **13**, 1287 (1958).
[10] I. A. Kurova and S. G. Kalashnikov, Soviet Phys.—Solid State **1**, 1353 (1960).
[11] P. Csavinszky, Phys. Rev. **119**, 1605 (1960).
[12] A. Miller and E. Abrahams, Phys. Rev. **120**, 745 (1960).
[13] R. J. Sladek and R. W. Keyes, Proceedings of the International Conference on Semiconductors, Prague, 1960 (to be published as Paper E3); Phys. Rev. **122**, 437 (1961).
[14] M. Pollak and T. H. Geballe, Proceedings of the International Conference on Semiconductors, Prague, 1960 (to be published as Paper F5).
[15] K. R. Atkins, R. Donovan, and R. H. Walmsley, Phys. Rev. **118**, 411 (1960).

should yield information about the hopping times provided the stimulus for the present work.

II. EXPERIMENTAL PROCEDURE

The real and the imaginary parts of the conductivity of a series of samples were evaluated from capacitance and loss-angle measurements. The measurements were made in decade increments over a frequency range from 10^2 to 10^5 cps with a precision capacitance bridge in connection with a high-sensitivity narrow-band amplifier. Capacitance changes as small as 0.01 $\mu\mu$f could be detected. The imaginary part of the conductance was reproducible to 3×10^{-14} ωohm^{-1}. The real part of conductance was reproducible to better than 20% at 10^{-13} ωohm^{-1} and this improved at higher conductances. The samples were disk-shaped, about 1 cm^2 in cross section and $\frac{1}{3}$ mm thick, so that conductivities of the order of 10^{-15} ω could be meaningfully measured. Impedances formed by various parallel connections of known capacitors and known high-value resistors were connected in place of the sample in order to check the capability of the system to measure conductances. The values of resistance obtained from the bridge measurements came close to the nominal values of the resistors used but were consistently about 15% lower.

The samples were prepared from a variety of Si crystals with different concentrations of group-III and group-V impurities. Considerable care was taken to determine the impurity concentrations. Essentially three different ways were used. (1) Advantage was taken of the fact that boron has a segregation coefficient of unity in silicon. Therefore the boron concentration throughout a crystal which was grown[16] with boron added to the melt was assumed to be constant. A group-V element was added to the melt during the growth as the majority impurity. The minority (p type) concentration was then evaluated from Hall or conductivity measurements at the seed end of the crystal. The majority carrier concentration was determined by probing the sample. (2) A series of crystals was grown using pile-activated indium as a minority impurity. The concentration of indium in the samples was determined by counting methods. The relative accuracy between samples is 3% except for the lowest counting rates. The absolute concentration is estimated to be determined to 10%.[17] (3) A series of n-type samples was prepared in which phosphorus was produced by transmutation of Si^{30} by low-energy neutron bombardment. The minority concentration was determined before bombardment. The phosphorus concentration can be determined from the total neutron flux, the relative abundance of Si^{30} and the known capture cross section for the reaction.[18] Tanenbaum has shown that the measured phosphorus concentration is in reasonable agreement with such a calculation provided that a simple annealing procedure is followed. The experimental results obtained from samples in this category are inconclusive and further experiments with neutron-bombarded samples are in progress.

Table I lists the samples measured, together with the kind and concentration of the majority and minority impurities. The method used for evaluating concentrations is indicated by (1), (2), or (3) in accordance with the above description.

Electrodes were applied to the flat surfaces of the disk-shaped sample in various ways to see whether contacts affected our measurements. It was found that simple gold contacts electroplated on lapped surfaces gave the same results as heavily doped N^+ contacts prepared by diffusing phosphorus into the surface. This is not surprising for ac measurements where the surface capacitance should provide a large series admittance irrespective of the conductance. However, it was surprising to find the dc conductivity unaffected by the surface treatment and consistent with the expected ionization energy in the appropriate temperature range indicating that the contact resistance was less than the

TABLE I. Sample characteristics.

Method of preparation[a] and sample no.		Crystal no.	Kind N_A	Kind N_D	Orient.	N_A (cm^{-3})	N_D (cm^{-3})
(1)	8	A78-25A	?	P	[111]	Small	1.5×10^{16}
(1)	9	215	B	P	[100]	0.8×10^{15}	1.4×10^{16}
(1)	9A	215	B	P	[100]	0.8×10^{15}	1.6×10^{16}
(1)	9B	215	B	P	[100]	0.8×10^{15}	1.2×10^{16}
(1)	12	215	B	P	[100]	0.8×10^{15}	1.1×10^{17}
(1)	13	215	B	P	[100]	0.8×10^{15}	2.7×10^{17}
(2)	16[b]	1X-562	In	As	[100]	1.3×10^{15}	1.15×10^{16}
(2)	17	1X-560	In	As	[111]	2.6×10^{15}	1.15×10^{16}
(2)	18	1X-561	In	P	[111]	6.2×10^{15}	2.3×10^{16}
(2)	19	1X-560	In	As	[111]	6.6×10^{15}	2.3×10^{16}
(2)	20	1X-560	In	As	[111]	4.9×10^{15}	1.7×10^{16}
(2)	21[b]	1X-562	In	As	[100]	2.1×10^{15}	1.7×10^{16}
(2)	22[b]	1X-562	In	As	[100]	6.2×10^{14}	6.8×10^{15}
(2)	23	1X-560	In	As	[111]	1.2×10^{15}	7.5×10^{15}
(2)	24	1X-561	In	P	[111]	1.2×10^{16}	4×10^{16}
(3)	25	FZ-I-190	In	P	[111]	5.0×10^{14}	3.1×10^{15}
(3)	26	FZ-I-193	In	P	[111]	8.3×10^{15}	3.1×10^{15}
(3)	27	FZ-I-193	In	P	[111]	5.0×10^{14}	6×10^{15}
(3)	28	FZ-I-193	In	P	[111]	7.0×10^{14}	1.4×10^{16}
(3)	29	FZ-I-193	In	P	[111]	1.05×10^{15}	1.4×10^{16}
(3)	31	FZ-I-193	In	P	[111]	8.3×10^{15}	1.4×10^{16}
(1)	32	1X-577	B	Sb	[100]	1.1×10^{15}	1.4×10^{16}
(1)	34	1X-577	B	Sb	[100]	1.1×10^{15}	3.2×10^{16}
(1)	35	1X-577	B	Sb	[100]	1.1×10^{15}	5.6×10^{16}
(1)	36	1X-578	B	Sb	[100]	5.2×10^{15}	1.5×10^{16}
(1)	37	1X-578	B	Sb	[100]	5.2×10^{15}	4.5×10^{16}
(1)	38	1X-579	B	As	[100]	3.8×10^{15}	1.4×10^{16}
(1)	39	1X-579	B	As	[100]	3.8×10^{15}	5.4×10^{16}

[a] For method of preparation for establishing compensation, see text.
[b] Samples from 1X-562 were nonlinear in response to applied voltage except at the lowest temperatures.

[16] We are indebted to P. E. Freeland for growing these crystals. The material supplied to the workers in reference 15 was also from some of these crystals.

[17] We are indebted to J. Struthers, P. Donovan, and W. Gibson for advice on the preparation and evaluation of these crystals. The indium was activated at the Brookhaven National Laboratory. The low-background counting was performed under contract by Tracerlab Inc., Waltham, Massachusetts.

[18] M. Tanenbaum, J. Electrochemical Society (to be published).

bulk resistance. Conductance due to surface leakage or other spurious effects was orders of magnitude below the lowest ac conductance measured. A further check for leakage paths was performed by control experiments on a high-purity undoped sample. No measurable losses were found at 4.2°K; the capacitance was independent of ω and could be fully accounted for by the dielectric constant of silicon.

Further evidence for interpreting the ac measurements as being due to impurity conduction and not spurious effects can be seen in Fig. 13, where the ac measurements are correlated with the dc measurements.

The samples (Fig. 2) were inserted as the dielectric of a condenser which was an integral part of a low-temperature sample holder. The holder was filled with a fraction of a mm of He gas at 4.2°K. Precautions were taken to prevent room-temperature radiation from reaching the sample. The contacts to the condenser were made by a coaxial arrangement. The outer conductor was grounded; the inner conductor was brought through a glass capillary tube. Stress could be applied via the glass tube to the sample. A spring arrangement was added to disconnect the central lead at the sample to determine the parallel conductance due to the holder.

The measurements were made over a temperature range from 1.2°K up to the ionization range where

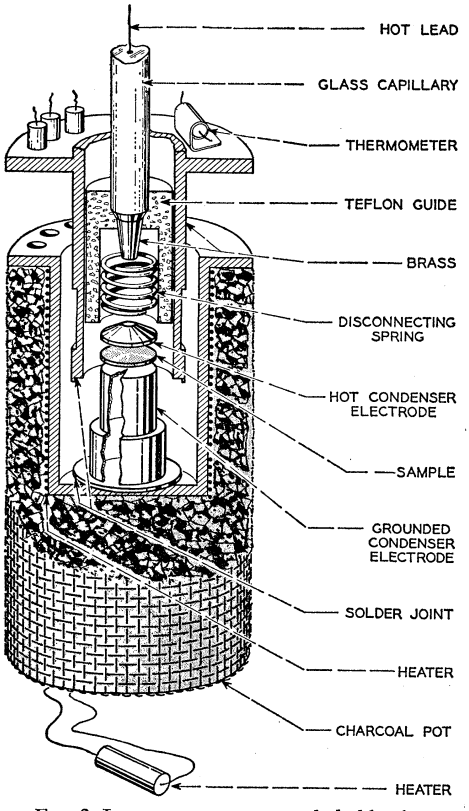

FIG. 2. Low-temperature sample holder for measuring low-frequency conductivity.

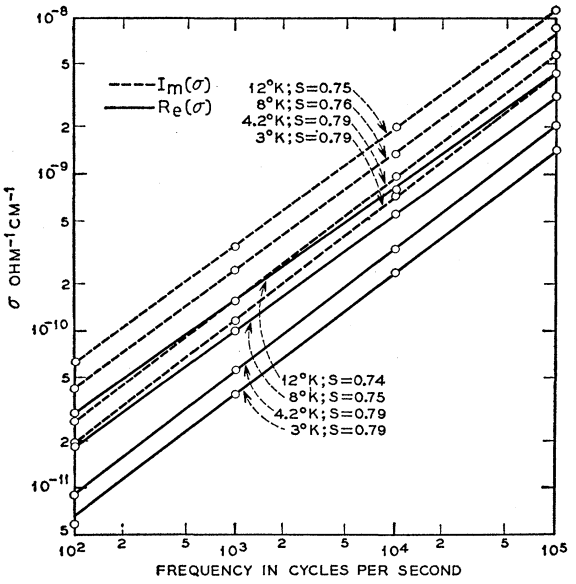

FIG. 3. Frequency dependence of the real and imaginary parts of the conductivity for sample 9.

conduction band electrons obscured the impurity conduction, usually about 25°K. Temperatures were measured with a carbon resistor. It was calibrated against the vapor pressures of hydrogen and helium and against a platinum thermometer previously calibrated by the National Bureau of Standards. The sample holder was surrounded by a charcoal pot and heater. Good temperature stability was available over the whole range.

III. EXPERIMENTAL RESULTS

For all the samples investigated, the conductivity increases with ω over the four decades measured according to the relation

$$\sigma_{ac} \equiv \sigma - \sigma_{dc} = A\omega^s, \tag{1}$$

where s is close to 0.8 and A is complex. Typical data are presented in Fig. 3. The slope s varies slowly from 0.79 at 3°K to 0.74 at 12°K. The Kramers-Kronig relation for Eq. (1) implies[19]

$$\mathrm{Im}(A)/\mathrm{Re}(A) = \tan(\tfrac{1}{2}s\pi). \tag{2}$$

The experimental data closely follow Eq. (2), indicating Eq. (1) holds at least a decade on either side of the frequency range actually measured. The magnitude of A varies with temperature, donor concentration, and degree of compensation.

Figure 4 shows the temperature dependence of $\mathrm{Re}(\sigma)$ of sample 8. The dc measurements represent transport by electrons ionized into the conduction band; there is no indication of dc impurity conduction. The ac results

[19] See, e.g., H. W. Bode, *Network Analysis and Feedback Amplifiers Design* (D. Van Nostrand Company, Inc., Princeton, New Jersey, 1945), p. 314.

coincide with the dc in the ionization range. At lower temperatures, however, there is an abrupt departure. $\mathrm{Re}(\sigma)$ is much less temperature dependent and rapidly becomes orders of magnitude greater than σ_{dc}. The $\omega^{0.8}$ dependence can be seen at any particular temperature. The plot also demonstrates the reproducibility of the measurements. The points are for two different runs made several weeks apart during which period the sample was removed from the holder. Figure 5 is for a much more heavily doped sample, 13, which shows dc impurity conduction. The plot is made against reciprocal temperature in order to demonstrate the activation energy (0.006 ev) for the dc impurity conduction. The increased slope at the very high temperature end represents the ionization range. The reduced slope at the low-temperature end of the dc curve may or may not be significant since it involved measurements at the limit of the sensitivity of the electrometer. The logarithmic scale is misleading in the region where the ac measurements seem to merge with the dc curve. Although the ac impurity conductivity becomes of the same order as the dc, it is always appreciably larger. The frequency dependence of the ac conductivity is $\omega^{0.9}$ for this sample, the largest exponent we have observed.

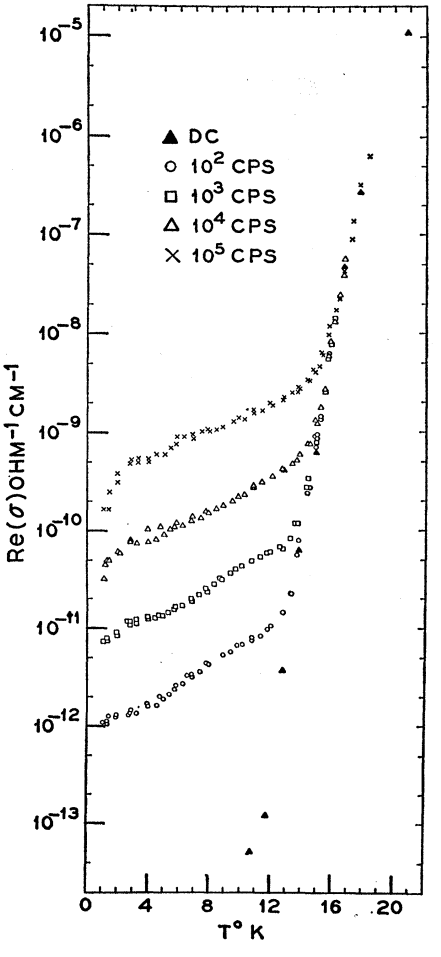

FIG. 4. Temperature dependence of the real part of the conductivity, and the dc conductivity for sample 8.

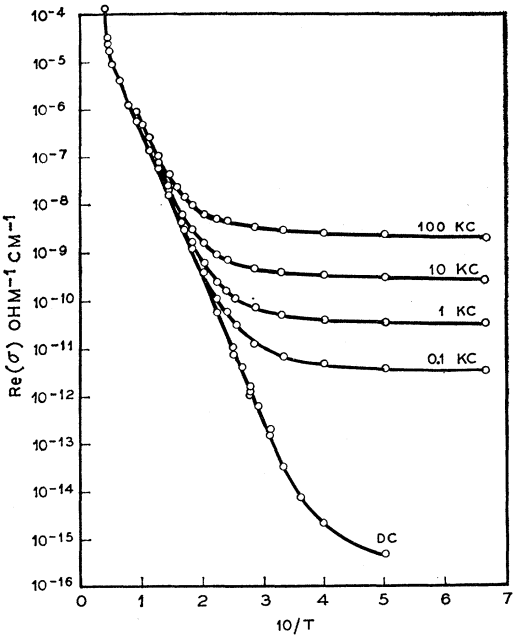

FIG. 5. Inverse temperature dependence of the real part of the conductivity, and the dc conductivity for sample 13.

The dependence upon majority impurity concentration is shown in Figs. 6 and 7. Figure 6 shows $\mathrm{Re}(\sigma)$ and $\mathrm{Im}(\sigma)$ for a series of samples with the same minority concentration. Three of the samples are from adjacent slices and have only slightly different majority concentrations, whereas the fourth, No. 12, has about an order of magnitude more. It can be seen that at the lowest measured temperatures the conductivity becomes almost independent of majority concentration, whereas at higher temperatures the dependence is pronounced. The high-temperature end of the $\mathrm{Re}(\sigma)$ plot again shows the onset of the ionization region. The curves representing sample 12 include an appreciable contribution from dc impurity conduction above 4°K. The resemblance between the real and imaginary parts of the conductivity where the dc conductivity is inappreciable is a consequence of the Kramers-Kronig relation. Figure 7 is a similar demonstration of the independence of σ upon majority impurity concentration at the lowest temperatures for other chemical impurities. $\mathrm{Re}(\sigma)$ at 100 cps is plotted for two additional sets of samples with arsenic and antimony majority impurities instead of phosphorus.

The dependence upon minority impurity concentration is shown in Figs. 8 and 9. Figure 8 shows the result of increasing the boron concentration from 1.1×10^{15} to 5.2×10^{15}. In contrast to the majority impurity case the dependence on the minority impurity concentration exists throughout the measured temperature range. The ratio of the conductivities of the two samples

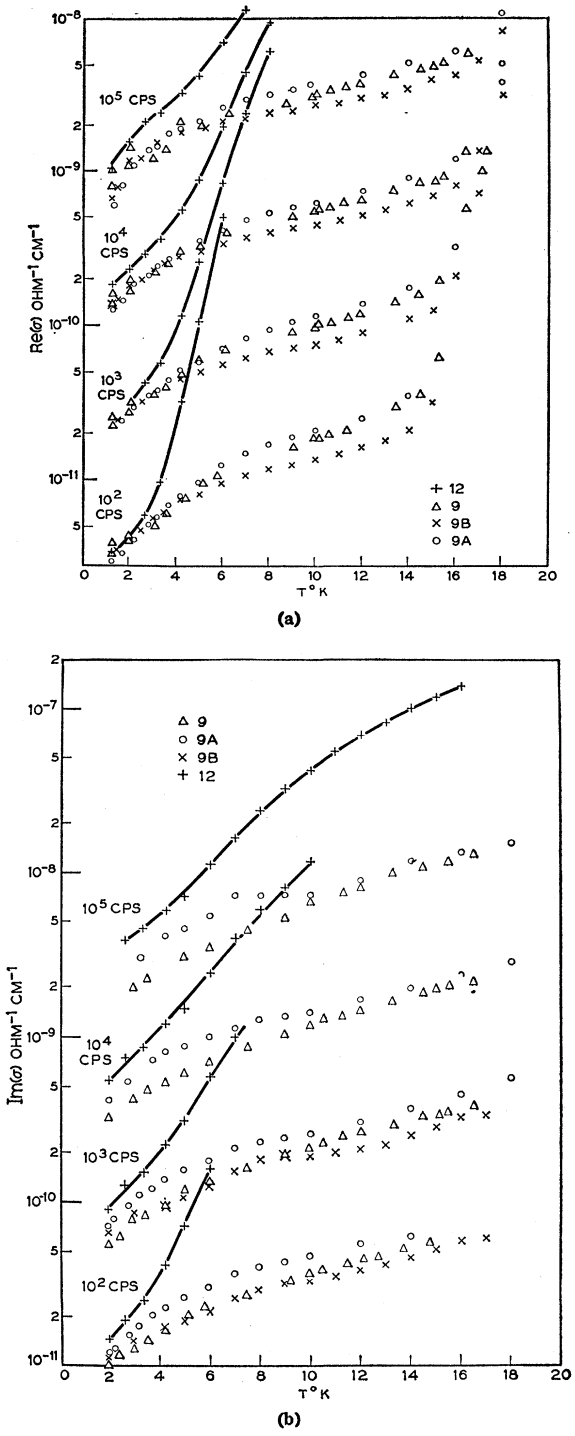

FIG. 6. The effect of varying majority concentration. Temperature dependence of the conductivity for a series of samples with the same boron concentration and varying concentrations of phosphorus donors. (a) The real part; (b) the imaginary part.

remains roughly the same and is almost equal to the minority concentration ratio. Figure 9 is for sample 9*B* for which three series of measurements were made with differing electrodes. The squares represent the initial measurements with gold-plated electrodes. The gold plating was removed (but incompletely) and phosphorus was diffused into the surface a depth of about 15 μ in order to form N^+ electrodes. Apparently a small amount of the much more rapidly diffusing residual gold entered the sample during the phosphorus diffusion. The increased compensation resulting from this diffused gold can be seen in the shift of the ionization range to higher temperatures (circles, Fig. 9). In the impurity conduction range the increased compensation causes increased conductivity. Finally, the N^+ contacts were lapped away and gold-plated electrodes again introduced. It is seen from the triangles, which

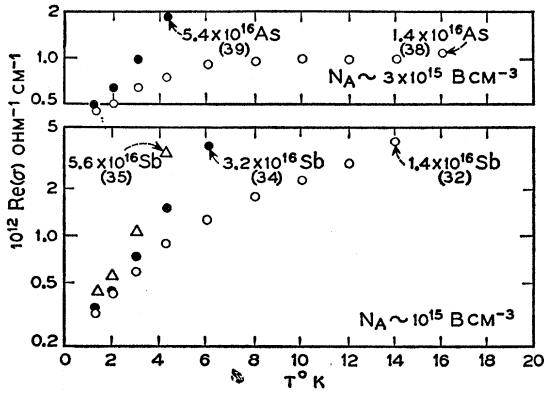

FIG. 7. The effect of varying majority concentration. Temperature dependence of the real part of the conductivity for samples containing the same boron concentrations and varying concentrations of arsenic or antimony as indicated. Sample numbers are indicated in parentheses.

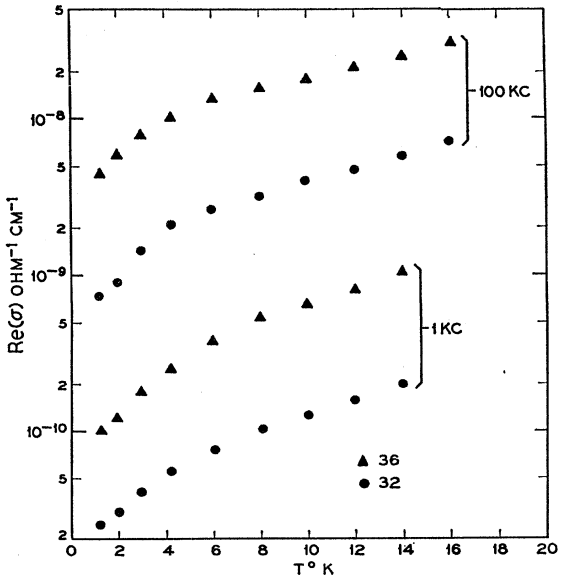

FIG. 8. The effect of varying minority concentration. Temperature dependence of the real part of the conductivity for samples with different boron and similar antimony concentrations.

represent the latter case, that the surface treatment hardly affected the results. Whatever difference is noticeable can probably be attributed to the incomplete homogenization of gold throughout the sample.

Figure 10 demonstrates the effect of minority and majority impurity concentration on $\mathrm{Re}(\sigma)$ at the lowest temperatures. The points all show a simple power law dependence on minority concentration which is almost unaffected by majority concentration. Only the kind of majority impurity seems to matter; the arsenic points lie below those for phosphorus and antimony. The slope of both curves is about 0.85 so that

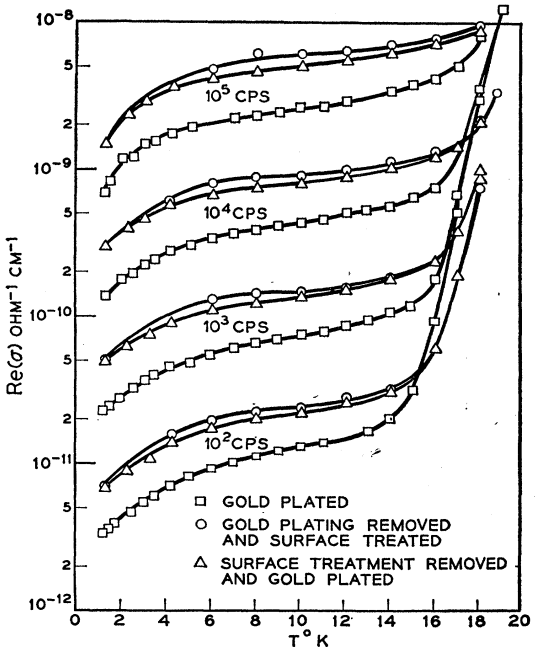

FIG. 9. The effect of contacts and gold diffusion on the real part of the conductivity for sample 9B.

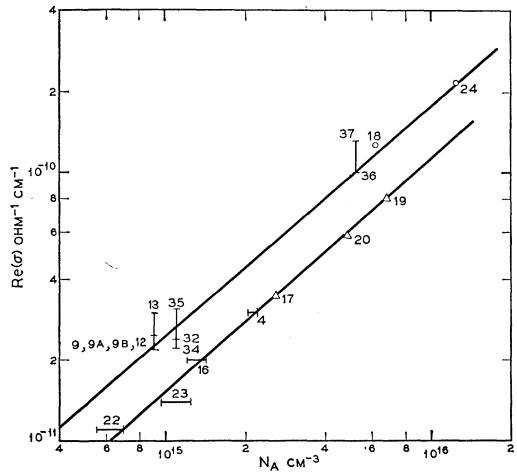

FIG. 10. Dependence of the real part of the conductivity at 10^3 cps on minority concentration at 1.2°K. Sample numbers are indicated.

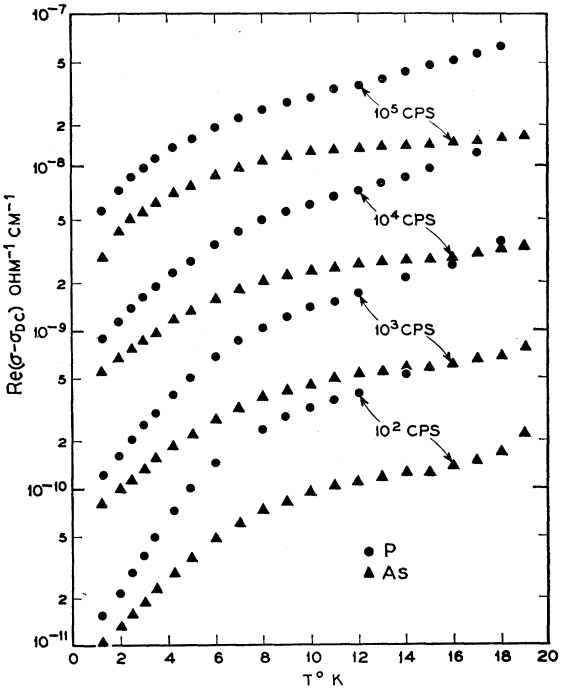

FIG. 11. Effect of different donors, phosphorus and arsenic, on the real part of the conductivity for samples with similar minority and majority concentrations.

the conductivity is almost proportional to the minority impurity concentration. Figure 11 for samples 18 and 19 shows the difference between arsenic- and phosphorus-doped samples over the whole temperature range. Both minority and majority concentrations for those samples are almost the same.

An attempt was made to detect effects of stress on the impurity conduction. Even under the most favorable conditions, namely, antimony-doped [100] samples, no effect was observed over the temperature range with stresses up to 5×10^7 d cm^{-2}.

IV. ANALYSIS OF THE RESULTS

In this section we present an analysis of our data. First of all we indicate how the direct measurements were converted into conductivity values. Following this a qualitative discussion is presented of what to expect when the Conwell-Mott impurity conduction model, established from steady field experiments, is subjected to alternating fields. A quantitative theory is given next. It expresses the conductivity in the form of an integral. Two methods are developed for comparing the theoretical expression with the experimental results. In both only the real part of the conductivity is treated because the imaginary part follows from the Kramers-Kronig relation. In the first method, integration is avoided by expressing the integrand itself in terms of experimentally measured quantities. This treatment, though subject to less approximation than

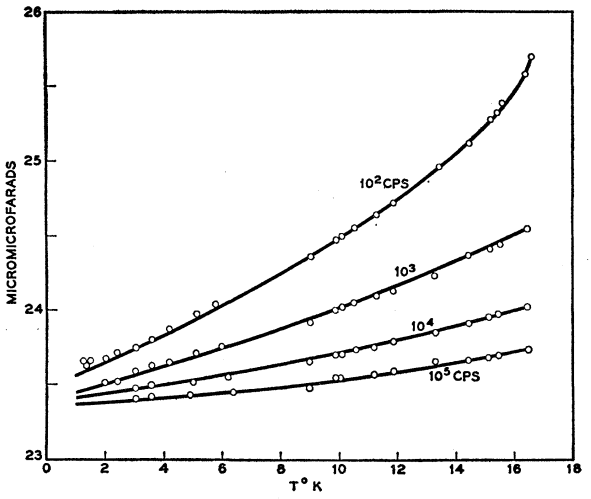

FIG. 12. Temperature dependence of the measured capacitance of the sample plus holder including frequency-independent parts.

the second one, requires the solution of an integral equation of the first kind. It is limited to certain functional dependences of $\mathrm{Re}(\sigma)$ on the frequency. The second method is an approximate integration and is more general. Both methods are used to compare the magnitude, frequency, and impurity concentration dependence of the theory with our experimental results. Finally, a way is outlined to use ac impurity conduction measurements for the determination of impurity distributions.

The direct measurements of the capacitance and the loss factor D are related to the relevant quantities $\mathrm{Re}(\sigma)$ and $\mathrm{Im}(\sigma)$. The real part is obtained directly from the capacitance and loss angle from the formula[20]

$$\mathrm{Re}(\sigma)=(\omega DC/1+D^2)(1-2DD_0)a/d,$$

where DD_0 is a correction tabulated in reference 20, and a/d is the geometric factor. To find the imaginary part, the capacitances due to the holder and the dielectric constant of Si have to be subtracted from the measured capacitance. It would be difficult to subtract these quantities by direct measurements as they account for almost all of the measured capacitance. Hence, either of the following procedures was followed: (1) Curves of capacitance versus temperature were drawn at different frequencies as in Fig. 12. $\mathrm{Log}[\mathrm{Re}(\sigma)]$ was plotted against ω at some arbitrary temperature to determine s in Eq. (1). As $\mathrm{Im}(\sigma)$ has to follow the same power law of ω as $\mathrm{Re}(\sigma)$ does (Kramers-Kronig), we have

$$[\mathrm{Im}\sigma(\omega_1)/\mathrm{Im}\sigma(\omega_2)]=(\omega_1/\omega_2)^s.$$

If the measured capacitance is $C(\omega)$ and the part to be subtracted C_0 (which can be assumed to be independent of ω), then

$$\frac{\mathrm{Im}\sigma(\omega_1)}{\mathrm{Im}\sigma(\omega_2)}\equiv\frac{\omega_1[C(\omega_1)-C_0]}{\omega_2[C(\omega_2)-C_0]}=(\omega_1/\omega_2)^s.$$

From this C_0 can be evaluated. (2) Another alternative to obtain C_0 is from Eq. (2), and the measurements of C and $\mathrm{Re}(\sigma)$ at any arbitrary temperature and frequency:

$$\mathrm{Im}[\sigma(\omega)]\equiv\omega[C(\omega)-C_0](a/d)=\tan(\tfrac{1}{2}s\pi)\mathrm{Re}[\sigma(\omega)].$$

The procedures correspond to the use of the Kramers-Kronig relation at one temperature to fit either the slope of $\mathrm{Im}(\sigma)$ between two frequencies or the magnitude of $\mathrm{Im}(\sigma)$ at one frequency. Our statement in Sec. III that the data follow Eq. (2) is not appreciably weakened.

Figure 13 demonstrates that the ac conductivity is correlated to the dc impurity conductivity. We expect therefore the same processes to be responsible for the dc and ac conductivities and treat our results in terms of the model of dc conductivity mentioned in the introduction.[21] It is indeed reasonable as such a model will provide us with a mechanism for producing ac conductivity much larger than a dc conductivity. One would expect the real part of the conductivity to be a monotonically increasing function of frequency. Macroscopically, the model implies a situation where the conductivity is finite at isolated parts of the crystal (near the ionized minorities) and vanishing in the other parts. The resulting conductance therefore consists of regions of finite conductivities coupled via capacities of the nonconducting parts. Such an arrangement of capacities and resistors must demonstrate an impedance which has a real part monotonically increasing with frequency. The macroscopic concept, however, does not apply to our problem as it involves the possibility of using Ohm's law for the regions of finite conductivity. This possibility does not exist on the scale of the neighborhood of a minority impurity.

Microscopically, if one considers an electron (or hole) jumping between two states with a certain statistical rate, the following statements will hold: at frequencies much lower than the jumping rate, equilibrium can be established much faster than the applied field changes. Hence the polarization will keep pace with the applied field without appreciable phase shift and the time derivative of the polarization will have a very small in-phase part, i.e., the real part of the conductivity will be very small. The magnitude of the polarization will gradually decrease with increasing frequency as it has less and less chance to keep up with the field variation. This decrease will never be faster than inversely proportional to frequency (i.e., propor-

[20] Operating instructions for General Radio type 716-C capacitance bridge.

[21] In this connection we might add that our experimental activation energies for dc conduction are not in as good agreement with dc theory as the cases treated by Miller and Abrahams (reference 12).

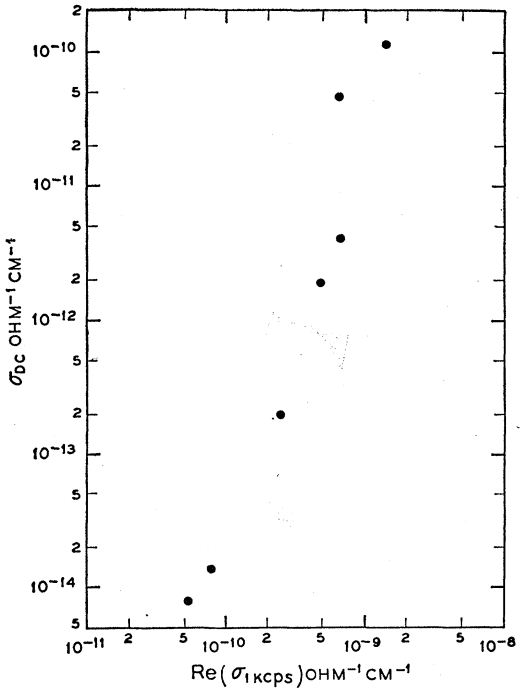

FIG. 13. Correlation (at 10°K) between the real part of the complex conducitvity (10^3 cps) and the dc conductivity.

tional to the rate of change of field). This inverse dependence will be approached at frequencies very high compared to hopping time, when the zero field equilibrium hardly has time to be disturbed. Because the conductance is proportional to ω times the polarization, the magnitude of the conductance has to be a nondecreasing function of ω. As the importance of the real part relative to the imaginary part becomes more important at higher frequencies, the real part of the conductance must also be an increasing function of frequency. If many noninteracting centers are involved, the total conductance will be a sum of increasing functions, again an increasing function of frequency. Hence, if the proposed model is to hold, the resulting real parts of the conductance should increase monotonically with frequency. Our results show such behavior over the measured frequency range. Tanaka,[22] working at higher frequencies, has results which indicate that the Re(σ) increases all the way to 9000 Mc/sec. It is thus seen that a model where hopping is localized in certain parts of the crystals has a frequency dependence in qualitative agreement with experiment.

In order to test the model, we shall compare our experimental results with the behavior expected from it in a more quantitative way. Disregarding the dc conduction, the current will be given (in rationalized units) by

$$j=\dot{p}, \tag{3}$$

where

$$p=V^{-1}\sum_i eX_i f_i, \tag{4}$$

e is the electronic charge, V is the volume over which the summation extends, X_i is the projection along the field direction of the separation of the ith majority impurity and the nearest minority impurity, and f_i is the occupancy probability (for a hole in n type) of the ith majority impurity, and is given by the solution of

$$\dot{f}_i=\sum_j W_{ij}f_j-\sum_j W_{ji}f_i, \tag{5}$$

together with the normalizing condition

$$V^{-1}\sum_j f_j=N_A. \tag{6}$$

The transition rates W_{ij} have been calculated by various workers.[9,12] The only difference between (5) and the results of Kasuya and Koide and of Miller and Abrahams is the omission of the exclusion factor $(1-f)$. We omit this factor because the occupancy of site j and nonoccupancy at site i are not independent events. Indeed, in the case of low compensation, the second is practically implied by the first. In the case of heavy compensation the situation is not very clear. Miller[23] estimated that including the factor in the latter case is a better approximation. Most of our samples are, however, in the low-compensation range and hence we shall write the equations in the form of Eq. (5).

For the general case Eq. (5) is very difficult to solve. Hence we shall idealize the situation by assuming that hopping occurs exclusively between pairs of majority impurities. This idealization is justified for most of our data in Appendix A. A second assumption that we shall make is that the jumping in a given pair is independent of the others, i.e., that the electric field at one hopping center is just the applied field, unaffected by the field produced by hopping in other pairs. This assumption is experimentally justified by the almost linear dependence of σ on minority impurity. We shall first investigate the conductivity of a cube of 1 cm^3 with n identical jumping centers. Each center consists of a pair of majority impurity atoms separated by an energy ΔE, distance r, and having all the same orientation θ with respect to the applied field (Fig. 1). Applying Eqs. (6) to (3) to this ensemble and substituting for i, j the indices 1, 2 which account for the two atoms of the n pairs, the equations acquire the form

$$f_1=1-f_2, \tag{7}$$

$$\dot{f}_1=W_{12}f_2-W_{21}f_1=-(W_{21}+W_{12})f_1+W_{12}, \tag{8}$$

$$p=ne(X_1f_1+X_2f_2)=ne(X_1-X_2)f_1+neX_2, \tag{9}$$

$$j=\dot{p}=ne(X_1-X_2)\dot{f}_1=ner\cos\theta\dot{f}_1. \tag{10}$$

We shall follow the behavior of f_i after a sudden application of a steady electric field, ϵ. This is given by the solution of Eq. (8) with proper boundary conditions, i.e., at $t=0$

$$f_1(0)=(e^{-\Delta E/kT}/1+e^{-\Delta E/kT}),$$

[22] S. Tanaka (private communication).

[23] A. Miller (private communication).

and at $t=\infty$

$$f_1(\infty)=(\alpha e^{-\Delta E/kT}/1+\alpha e^{-\Delta E/kt}) \quad \text{with}$$
$$\alpha=e^{(-\epsilon er\cos\theta/kT)}\approx 1-(\epsilon er\cos\theta/kT).$$

The solution is

$$f_1(t)=f_1(0)+[f_1(\infty)-f_1(0)](1-e^{-Kt}),$$

with

$$K\equiv\tau^{-1}=W_{12}+W_{21}.$$

From the symmetry of the problem, half of the pairs for which a hop occurs in the direction of ϵ will go to states which are higher in energy at zero field, and half to states lower in energy. This can be taken into account by changing indices for half the pairs, and gives

$$j(t)=\frac{1}{4}nr\cos\theta e\tau^{-1}\frac{1}{\cosh^2(\Delta E/2kT)}\frac{e\epsilon r\cos\theta}{kT}e^{-t/\tau}.$$

Transforming into the frequency-dependent form by the Laplace method:

$$\frac{j(\omega)}{\epsilon(\omega)}=\frac{1}{4}nr^2\cos^2\theta e^2\frac{1}{kT\cosh^2(\Delta E/2kT)}$$
$$\times\tau^{-1}\left[\frac{\omega^2\tau^2}{1+\omega^2\tau^2}+i\frac{\omega\tau}{1+\omega^2\tau^2}\right].$$

We have to consider now that the pairs are actually not identical but are randomly arranged. As we assume that there is no interaction between hopping centers, the total conductivity will be an additive function of the contributions from all pairs. We can therefore employ a straightforward integration process weighting the partial contributions from different pairs according to their probability of occurrence. The integration has to be done over ΔE, r, and θ. The last part is simple and yields

$$d\sigma(r,\Delta E,\omega)=\frac{1}{12}dp(r,\Delta E)N_A\frac{e^2}{kT}$$
$$\times r^2\tau^{-1}\left[\frac{\omega^2\tau^2}{1+\omega^2\tau^2}+i\frac{\omega\tau}{1+\omega^2\tau^2}\right]\frac{1}{\cosh^2(\Delta E/2kT)};$$

$dp(r,\Delta E)$ is the number of pairs of spacing r and energy separation ΔE; N_A is the total density of pairs and is equal to the number of acceptors. The equation is in agreement with one obtained by Lax[24] using the Nyquist theorem and a generalized theory of the ac diffusion constant. The averaging over ΔE and r is much more involved. Properly, as both ΔE and r influence σ, one should integrate over the distribution of pairs using the whole energy difference and distance spectra. The resulting integral is prohibitive.

The strong influence of ΔE on σ is through the factor $\cosh^2(\Delta E/2kT)$, while τ itself is not a very strong function of ΔE. It is, however, an exponential of the distance. When ΔE is not much larger than kT, $\cosh^2(\Delta E/2kT)$ is close to unity, and hence at high enough temperature we can probably neglect the ΔE dependence. With such an assumption, $\mathrm{Re}(\sigma)$ becomes

$$\mathrm{Re}(\sigma)=\frac{1}{12}N_AN_D\frac{e^2}{kT}\int r^2\tau^{-1}\frac{(\omega\tau)^2}{1+(\omega\tau)^2}4\pi r^2dr, \quad (11)$$

since for random impurity distribution

$$dp(r,\Delta E)=4\pi N_Dr^2dr.$$

TABLE II. Concentration dependence at 20°K for $\mathrm{Re}(\sigma)$ at 100 kc/sec for arsenic majority atoms.

Sample no.	N_AN_D	$\mathrm{Re}(\sigma)$	$\mathrm{Re}(\sigma)/N_AN_D$
17	3.0×10^{31}	4.2×10^{-9}	1.4×10^{-40}
20	8.6×10^{31}	11×10^{-9}	1.3×10^{-40}
23	0.92×10^{31}	1.3×10^{-9}	1.4×10^{-40}

A few important results are apparent without explicit integration. (1) The conductivity should vary linearly with majority concentration as well as with minority concentration. This seems to be fairly well borne out at higher temperatures as illustrated in Table II. At low temperatures, however, the experimental results indicate that $\mathrm{Re}(\sigma)$ is almost independent of majority impurities. However, at these temperatures it is no longer justified to neglect averaging over ΔE. We are indebted to M. Lax for attempts to evaluate the behavior of $\mathrm{Re}(\sigma)$. His preliminary results indicate that the majority dependence should indeed be less than linear at those temperatures; however, they do not predict a lack of sensitivity to majority impurities to the degree observed.[25] Possibly the results could be explained by a nonrandom distribution of the distance between minority impurities and nearest neighbor majority impurities caused perhaps by Coulombic forces among the ionized impurities during crystallization. The neutron-bombarded samples may shed some light on this, as the distribution in these samples is guaranteed to be random. Unfortunately, our few experiments in this field are inconclusive; more work is in progress. At this point we shall satisfy ourselves therefore with the statement that the low-temperature behavior is not well understood. It may, however, become a useful tool for evaluating minority concentrations because of the insensitivity to majority impurities.

An interesting property of Eq. (11) is the sharp-peaked feature of the integrand with respect to r, since τ depends on r exponentially [Eq. (13a)]. It means that the contributions to $\mathrm{Re}(\sigma)$ come from pairs whose

[24] M. Lax (to be published).

[25] The decreased majority dependence at low temperatures may be qualitatively understood. Increasing the majority concentration will decrease the average minority to nearest majority atom distances and hence increase ΔE.

spacing is at some particular distance. This suggests that if the theory proves to be adequate, experiments similar to ours may be useful for determining the distribution of spacing among the majority impurities.

In analyzing our results we shall assume that the experimental results can be expressed as a superposition of responses corresponding to relaxation processes with various relaxation times, i.e.,

$$j=\epsilon\int_0^\infty G(\tau)e^{-t/\tau}d\tau,$$

or in the frequency-dependent form,

$$\mathrm{Re}(\sigma)=\int_0^\infty G(\tau)(\omega^2\tau^2/1+\omega^2\tau^2)d\tau.$$

This expression then can be compared to experimental results, Eq. (1), on one hand and to the theoretical predictions, Eq. (11), on the other:

$$\omega^{0.8}\mathrm{Re}(A)=\int_0^\infty G(\tau)\frac{\omega^2\tau^2}{1+\omega^2\tau^2}d\tau$$
$$=\frac{4\pi}{12}\frac{e^2}{kT}N_AN_D\int_0^\infty r^4\tau^{-1}\frac{\omega^2\tau^2}{1+\omega^2\tau^2}dr. \quad (12)$$

The left and center parts present an integral equation from which $G(\tau)$ can be evaluated in terms of the measured A:

$$G(\tau)=[2A/\Gamma(0.6)\Gamma(0.4)]\tau^{-1.8}=0.6A\tau^{-1.8}.$$

Here and in the following, A stands for $\mathrm{Re}(A)$.

Substituting $G(\tau)$ into Eq. (12) and comparing the two right-hand integrands, we obtain

$$0.6A\tau^{-0.8}d\tau=\frac{4\pi}{12}N_DN_A\frac{e^2}{kT}r^4dr. \quad (13)$$

Using Miller and Abrahams' theory[12] for the transition rates, one obtains

$$\tau\cong 5\times10^{-13}(r/a)^{-\frac{3}{2}}e^{2r/a}\tanh(\Delta E/2kT). \quad (13a)$$

Substituting into (13), we have

$$3.4\times10^4Ae^{0.4r/a}(r/a)^{-0.3}[\tanh(\Delta E/2kT)]^{0.2}$$
$$=3.3N_DN_Ar^4e^2/kT. \quad (14)$$

TABLE III. Dependence of Eq. (14) on frequency parameter (r/a) (using experimental value of A for sample 9 at 10°K).

Frequency (cps)	r/a	Left side of Eq. (14)	Right side of Eq. (14)	Ratios Col. 4 to Col. 3
10^2	12.8	30.1×10^{-8}	35.2×10^{-8}	1.17
10^3	11.6	19.4×10^{-8}	23.7×10^{-8}	1.22
10^4	10.3	12.2×10^{-8}	14.7×10^{-8}	1.20
10^5	9.1	7.5×10^{-8}	8.9×10^{-8}	1.19

TABLE IV. Calculated and experimental values of A of Eq. (1).

Sample no.	10^8a (cm)[a]	T (°K)	$10^{13}A_{\mathrm{calc}}$	$10^{13}A_{\mathrm{exp}}$
9	21.1	5	2.7	0.5
		10	1.3	1.1
		15	0.9	1.4
17	20	5	5.8	0.56
		10	2.9	0.75
		15	1.9	0.78
		20	1.4	0.8
32	22	5	4.3	0.6
		10	2.2	1.1
		15	1.4	1.8

[a] See Table I, reference 12.

The factor $[\tanh(\Delta E/2kT)]^{0.2}$ is near unity throughout our temperature range. Obviously, this equality does not hold universally, as the r dependence on both sides is different. However, as we pointed out before, the integrand contributes appreciably to the integral only over a small region of r, dependent on the ω at which the conductivity is evaluated. Hence we shall demand that (14) hold only over such region of r as will contribute to our measured results, i.e., to r corresponding to frequencies from 10^2 to 10^5 cps. One discrepancy is immediately seen between the quantity A and the predicted behavior. While A is found experimentally to increase with temperature, it should decrease as $1/T$, according to Eq. (14). This discrepancy may mean that the activation term which has been neglected is still important even at the highest temperatures which could be achieved experimentally. If that is the case, the experimental values of A should lie below those predicted by Eq. (14).

To compare the magnitudes, we evaluate the range of r for which the comparison should be valid. The values of r/a for which the integrand has a large contribution are as follows: for $f=10^2$ cps, $r/a=13$; for $f=10^5$ cps, $r/a=9$. For those values of r/a the two sides of Eq. (14) are given in Table III, corresponding to parameters of sample 9 at 10°K. The table demonstrates by virtue of the constancy of the right-hand column that the $\omega^{0.8}$ dependence has been properly accounted for. The theoretical magnitude is seen to exceed the experimental by a factor of about 1.2.

Table IV provides a more complete comparison of experiment and theory. The values here are tabulated in a somewhat different way than in Table III. A is computed from Eq. (14) at $r/a=13$ at different temperatures and compared to the measured value. The agreement is seen to improve with increasing temperature, as expected. Figure 14 is a plot of the behavior of the two sides of Eq. (14). Both curves are normalized at their value of $r/a=11$. This is where the r/a value corresponds to the center of our frequency range. It turns out to be also roughly where the two curves have the same slope. We see that in our frequency range the

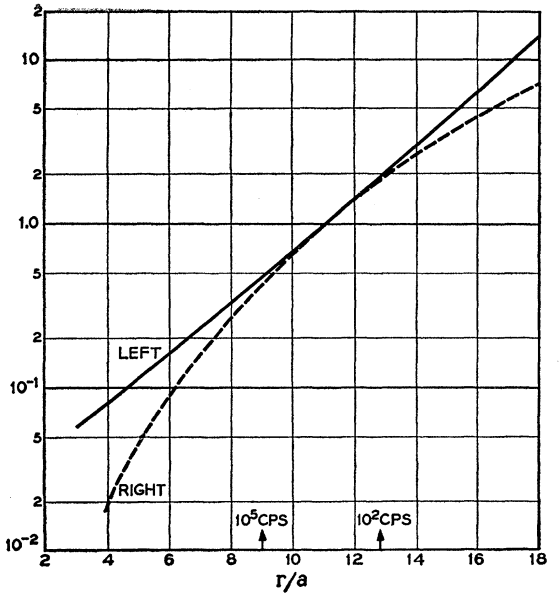

FIG. 14. Behavior of the left- and right-hand sides of Eq. (14) as a function of the pair spacing.

two curves are very close to each other. This means that the frequency behavior of our experimental data corresponds very well to that predicted by the above simple theory. According to the figure, we should expect the validity of the relationships $\mathrm{Re}(\sigma)=A\omega^{0.8}$ to cease gradually as we leave our frequency range. The slope of the curve representing the left side of Eq. (14) is almost proportional to $1-s$, hence for higher values of s the two curves will be tangent to each other at higher values of r/a, i.e., at values corresponding to lower frequencies, and vice versa. This means that for lower frequencies the frequency dependence should be more pronounced than $\omega^{0.8}$ and less pronounced for higher frequencies.

It is of interest to use a different method to evaluate the experimental results. In doing this we follow a similar procedure to that used by Lax.[25] Although some approximations will be used in the following, which were not used in the previous method, the results will follow directly in terms of the conductivity, rather than of the constant A and hence will be valid more generally than for an $A\omega^s$ dependence.

As was said before, the integrand of Eq. (11) is sharply peaked around a certain value of r which depends on ω. The integral can be put into the form

$$\sigma(\omega)=\frac{4\pi}{12}\omega N_A N_D\frac{e^2}{kT}a^5\int_0^\infty\left(\frac{r}{a}\right)^4\frac{d(r/a)}{\varphi(r)e^{2r/a}+\varphi^{-1}(r)e^{-2r/a}},$$

where from Eq. (13a)

$$\varphi(r)\equiv\tau\omega e^{-2r/a}=5\times10^{-13}(r/a)^{-\frac{3}{2}}\omega\tanh(\Delta E/2kT).$$

The terms responsible for the peaked character of the integrand are the exponentials in r; the other functions of r are relatively slowly varying, hence we can write approximately

$$\sigma(\omega)=\frac{4\pi}{12}\omega N_A N_D\frac{e^2}{kT}a^5(r_{\max}/a)^4\times\int_0^\infty\frac{d(r/a)}{\varphi(r_{\max})e^{2r/a}+[\varphi(r_{\max})e^{2r/a}]^{-1}},$$

where $r_{\max}$ refers to r at which the integrand has its maximum. The last integral can readily be evaluated. The value for $r_{\max}$ can be found from the approximate condition $\varphi(r_{\max})e^{2r_{\max}/a}=1$. Using $\ln(r/a)\cong[(r-a)/r]+\frac{1}{2}[(r-a)/r]^2+\cdots$ and $r/a+a/r\approx r/a$, the result is

$$\mathrm{Re}(\sigma)=(4\pi/12)N_D N_A(e^2/kT)(14.8-\tfrac{1}{2}\ln\omega)^4(a^5/2)\times\omega\{\pi/2-\arctan[5.5\times10^{-13}\times\omega(14.8-\tfrac{1}{2}\ln\omega)^{\frac{3}{2}}\tanh(\Delta E/2kT)]\}. \quad (15)$$

In Eq. (15), ω is to be given in sec^{-1}. The arctan can be neglected for frequencies below 10^{12} cps. Figure 15 shows the frequency dependence of $\mathrm{Re}(\sigma)$ from 1 to 10^7 cps. In our frequency range the curve follows very closely an $\omega^{0.8}$ dependence. Figure 16 shows a comparison of $\mathrm{Re}(\sigma)$ values for measured and calculated results using Eq. (15). The numerical agreement is reasonably good and the frequency response agreement very good, if, as was assumed, the distribution of impurities is random, i.e., $dN=4\pi r^2N_D dr$. Actually, because of the nature of the integral the frequency dependence should provide a good tool for measuring the distribution of impurities, i.e., the r dependence of dN/dr. With the

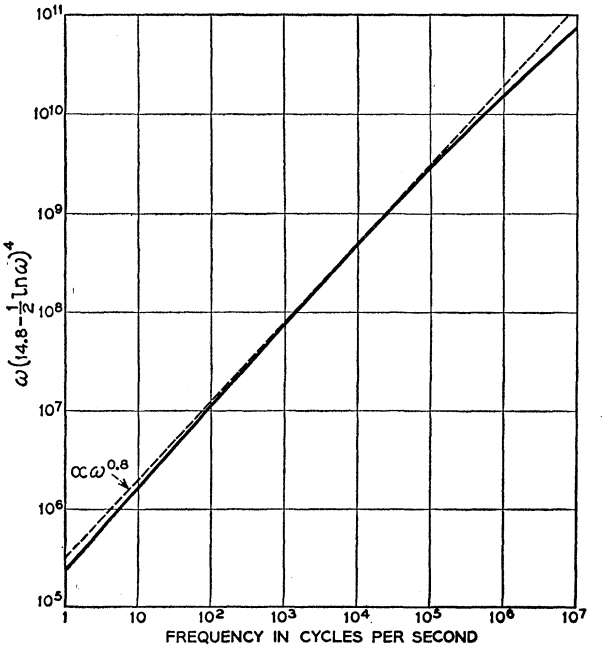

FIG. 15. Comparison of the frequency dependence of the real part of the conductivity predicted by Eq. (15) with experiment.

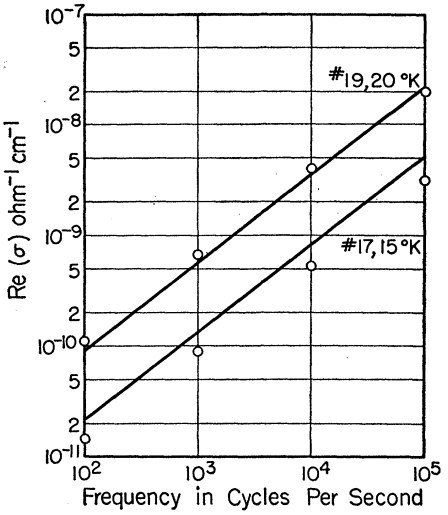

FIG. 16. Comparison of the real part of the conductivity calculated from Eq. (15) (solid lines) with experiment (circles).

same process as above, using $dN/dr=N(r)$ instead of $4\pi r^2N_D$, we obtain

$$N(r)=[48kT/\pi N_A e^2a^3\omega(14.8-\tfrac{1}{2}\ln\omega)^2]\mathrm{Re}[\sigma(\omega)].$$

where r is related to ω by $r=a(14.8-\frac{1}{2}\ln\omega)$.

The result should give an idea about the relative abundance of pairs at different distances. The absolute magnitude is unfortunately difficult to obtain, as the numerical agreement between experiments and theory is not sufficiently good. If a large enough frequency range is covered, the magnitude could possibly be obtained from the condition

$$\int_0^\infty N(r)dr=N_D.$$

Our experimental results agree well with a random distribution of pair spacing, as the experimentally observed frequency dependence is predicted when an r^2 dependence is assumed for $N(r)$. It should be made clear that this does not bear directly on the previous statement made that the lack of dependence of σ on the majority impurities at very low temperatures could have something to do with nonrandom distribution of impurities. Whereas the latter refers to the distribution of minority to nearest majority distances, the former is a measure of majority to majority distances.

ACKNOWLEDGMENTS

We are grateful to G. W. Hull, Jr., for his patience and care in carrying out many of the experimental details. We would like to thank Melvin Lax for many fruitful discussions carried out during the course of this work. We also acknowledge with pleasure the critical reading of the manuscript by T. D. Holstein and A. Miller. We would also like to thank P. W. Anderson for originally pointing out that the hopping mechanism should contribute to the low-frequency dielectric constant, and A. Miller and E. Abrahams for discussing with us their theoretical results.

APPENDIX A

In this appendix we demonstrate that for most of our measurements the model of pairs should be a very good approximation to the actual situation where hopping will occur among more than two majority impurities. Consider a formation of three impurities 1, 2, 3 with impurity 1, for instance, being deepest in the potential well. The effect of atom 2 on the hopping rate 1–3 is to reduce this rate by the relative amount of time the electron (hole) spends at atom 2. This reduction is partially compensated by occasional jumps from 2 to 3. If we considered the pairs 1–2 and 1–3 as independent pairs, the effect of the one atom on the hopping rate between the other two would be completely neglected. If, on the other hand, we assume that the presence of atom 2 completely eliminates the hopping between atoms 1 and 3, we overestimate the influence of atom 2. The true situation should therefore lie in between these two extremes (probably much closer to the first). The first case can be accounted for with a pair model where the distribution of distances between all atoms should be used, i.e., $dp=4\pi N_D r^2dr$ as the probability of a pair having the separation r. The second case can also be accounted for with a pair model, but the distribution of separations of nearest neighbors only should be used now, i.e., $dp=4\pi N_D r^2\times\exp[-(4\pi N_D r^3)/3]dr$. The two distributions differ by the factor $\exp[-(4\pi N_D r^3)/3]$. This factor closely resembles a step function equal to unity for $r<[3/(4\pi N_D)]^{\frac{1}{3}}$ and to zero for $r>[3/(4\pi N_D)]^{\frac{1}{3}}$. For $r<[3/(4\pi N_D)]^{\frac{1}{3}}$ the two cases give therefore the same result and the actual situation which is intermediate between the two must also give the same result. Hence the pair model used is a good one at least for $r<[3/(4\pi N_D)]^{\frac{1}{3}}$. Our largest r used, for antimony at 100 cps, is $13\times22\text{A}=286\text{A}$. For antimony, therefore, the pair model should be good at least up to concentrations $N_D=3/(4\pi r^3)\approx10^{16}$ cm^{-3} and slightly higher for phosphorus and arsenic. It would be of interest to examine the results on samples 11, 12, and 35 in order to see whether the theory actually breaks down for higher impurity concentrations. Unfortunately, in the temperature range where the theory should be valid, the dc contribution to the conductivity is appreciable and we do not believe our measurements to be sufficiently accurate to obtain σ_{ac} by subtracting σ_{dc} from $\sigma_{measured}$.

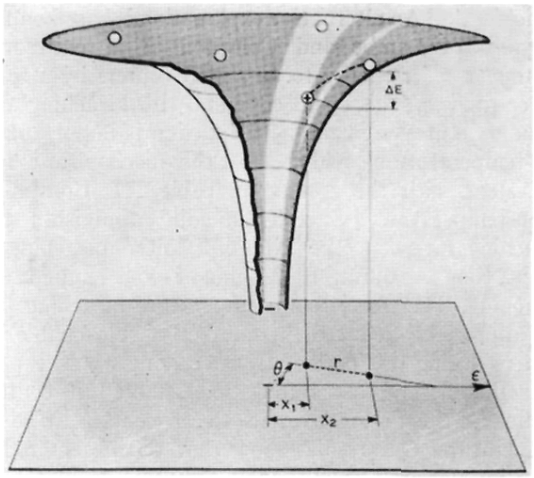

FIG. 1. A two-dimensional representation of the Mott-Conwell model for impurity conduction. The upper half of the figure shows a random distribution of majority donor atoms in the Coulombic potential of the negatively charged acceptor. The charge distribution can respond to an applied field ϵ by an electron hop (with energy increase ΔE) from an adjacent uncharged donor to the charged donor as indicated by the dashed line. The lower half of the figure shows the impurity atoms projected on the plane containing the field ϵ and illustrates the notation used in the text. Ionized donors and acceptors are represented by plus and minus signs; neutral donors by open circles.